



Subchondral bone expansion in advanced knee osteoarthritis: Relation with radiographic severity and role in surgical decision-making

Wei Wang^{a,1}, Tianshu Jiang^{a,1}, Jiang Zhang^b, Jun Liu^a, Lok Chun Chan^{a,c}, Mengqi Lin^d, Jia Li^e, Changhai Ding^{f,g}, Kwong Yuen Chiu^h, Henry Fu^h, Ping Keung Chan^h, Chunyi Wen^{a,c,*}

^a Department of Biomedical Engineering, Faculty of Engineering, The Hong Kong Polytechnic University, Hong Kong SAR, China

^b Department of Health Technology and Informatics, Faculty of Health and Social Sciences, The Hong Kong Polytechnic University, Hong Kong SAR, China

^c Research Institute of Smart Ageing, The Hong Kong Polytechnic University, Hong Kong SAR, China

^d Department of Software Engineering, Faculty of Electrical and Computer Engineering, Jilin Jianzhu University, Changchun, China

^e Department of Orthopedics, Nanfang Hospital, Southern Medical University, Guangzhou, China

^f Clinical Research Center, Zhujiang Hospital, Southern Medical University, Guangzhou, China

^g Menzies Institute for Medical Research, University of Tasmania, Hobart, Australia

^h Department of Orthopaedics and Traumatology, The University of Hong Kong, Hong Kong SAR, China

ARTICLE INFO

Handling Editor: H Madry

Keywords:

Knee osteoarthritis
Computed tomography
Subchondral bone
Joint space narrowing
Surgical decision-making

ABSTRACT

Background: Joint space width (JSW) is a traditional imaging marker for knee osteoarthritis (OA) severity, but it lacks sensitivity in advanced cases. We propose tibial subchondral bone area (TSBA), a new CT imaging marker to explore its relationship with OA radiographic severity, and to test its performance for classifying surgical decisions between unicompartmental knee arthroplasty (UKA) and total knee arthroplasty (TKA) compared to JSW.

Methods: We collected clinical, radiograph, and CT data from 182 patients who underwent primary knee arthroplasty (73 UKA, 109 TKA). The radiographic severity was scored using Kellgren-Lawrence (KL) grading system. TSBA and JSW were extracted from 3D CT-reconstruction model. We used independent *t*-test to investigate the relationship between TSBA and KL grade, and binary logistic regression to identify factors associated with TKA risk. The accuracy of TSBA, JSW and established classification model in differentiating between UKA and TKA was assessed using AUC.

Results: All parameters exhibited inter- and intra-class coefficients greater than 0.966. Patients with KL grade 4 had significantly larger TSBA than those with KL grade 3. TSBA (0.708 of AUC) was superior to minimal/average JSW (0.547/0.554 of AUC) associated with the risk of receiving TKA. Medial TSBA, together with gender and Knee Society Knee Score, emerged as independent classification factors in multivariate analysis. The overall AUC of composite model for surgical decision-making was 0.822.

Conclusion: Tibial subchondral bone area is an independent imaging marker for radiographic severity, and is superior to JSW for surgical decision-making between UKA and TKA in advanced OA patients.

1. Introduction

Knee osteoarthritis (OA) is a prevalent degenerative disease worldwide and a leading cause of joint pain and disability [1]. Loss of articular cartilage, which serves as a cushion for joint movement, is a hallmark of OA [2], and currently, there is no cure once damage occurs. For advanced knee OA patients, knee arthroplasty is the last but effective resort to relieve pain and restore function, with total knee arthroplasty (TKA)

being the traditional option [3]. Over the past few decades, unicompartmental knee arthroplasty (UKA) has been increasingly used in cases where damage is limited to one anatomic compartment due to its less invasive nature, shorter recovery time, and better postoperative function [4]. The current surgical decision between TKA and UKA partly relies on radiographical findings like the narrowing of joint space width (JSW). However, studies have demonstrated that for advanced knee OA, JSW has limited sensitivity to assess structural severity [5,6]. Therefore,

* Corresponding author. Department of Biomedical Engineering, Faculty of Engineering, The Hong Kong Polytechnic University ST417, 4/F, Block S, Hong Kong SAR, China.

E-mail address: chunyi.wen@polyu.edu.hk (C. Wen).

¹ These authors contributed equally to this work.

<https://doi.org/10.1016/j.ocarto.2024.100461>

Received 8 November 2023; Received in revised form 28 February 2024; Accepted 11 March 2024

2665-9131/© 2024 The Author(s). Published by Elsevier Ltd on behalf of Osteoarthritis Research Society International (OARSI). This is an open access article under the CC BY-NC-ND license (<http://creativecommons.org/licenses/by-nc-nd/4.0/>).

there is a growing need to develop a new imaging marker to accurately assess the degree of structural damage in advanced-stage knee OA and provide quantitative evidence for surgeons when making surgical decisions.

JSW is a conventional imaging marker for evaluating the severity of knee OA [7] but might underestimate cartilage degeneration in advanced cases. It is measured as the distance between the margins of the femur and tibia in anteroposterior (AP) knee radiographs to indicate cartilage loss indirectly [8]. JSW is a component of several scoring systems for knee OA, including the commonly used Kellgren-Lawrence (KL) grading system, where radiographic severity is assigned from KL grade 0 to KL grade 4 with the narrowing of JSW [9]. However, researchers have reported that in up to 50% of cases undergoing primary TKA, the degree of articular cartilage damage was more severe than the preoperative KL grade [6]. Additionally, a 30-month follow-up MRI examination found the continued occurrence of degenerative lesions such as cartilage loss, effusion, and synovitis in KL grade 4 knees [10].

The subchondral bone undergoes remarkable remodelling during OA progression and plays a crucial role in supporting the overlying cartilage [11]. Previously, the subchondral bone size measured in MRI cross-sectional slices was found to expand with the increasing extent of cartilage loss [12,13]. In the other cohort study, Researchers used MRI to follow up on the size of subchondral bone in osteoarthritic knees with different KL grades [14]. They found that patients with higher KL grades tended to have a greater change in subchondral bone size. Recently, Gary and colleagues proposed a shape measure of subchondral bone length in MRI sagittal slices (defined as SBL) based on the extent of overlying cartilage. They showed that SBL was associated with the risk of future knee replacement surgery [15]. However, MRI suffers from limitations such as distortion and poor bone contrast due to magnetic field inhomogeneities and limited scan time [16,17]. Furthermore, given the worn-out cartilage and continued activity of subchondral bone [18], MRI may not be the optimal imaging modality for accurately assessing the subchondral bone shape in advanced-stage OA [19].

CT imaging provides high-resolution images of bone structures and has become a useful tool for preoperative planning in knee joint replacement surgery [20], while its potential to assess disease severity and assist in surgical decision-making remains unclear. Therefore, we developed the tibial subchondral bone area (TSBA) as a new preoperative imaging marker based on 3D CT-reconstruction bone model to characterise tibial subchondral bone expansion. The following research questions were asked: 1) Is the value of TSBA related to OA radiographic severity in advanced OA patients? 2) Can TSBA perform better in classifying surgical decisions between UKA and TKA compared to JSW? 3) Can TSBA provide surgeons complementary information independent of clinical covariates in surgical decision-making?

2. Method

2.1. Patient population

The ethical approval of this study was obtained from the Hospital Authority of Hong Kong (approval number UW 22–090). A retrospective search of the Queen Mary Hospital's dataset was conducted to retrieve patients who underwent primary knee arthroplasty using the Robotic-Arm Assisted Surgery system between January 2019 and January 2022. The surgical decision for UKA fulfilled the inclusion criteria delineated by Kozin & Scott [21,22] (details are described in [Supplementary table S1](#)). A total of 200 patients were enrolled in this study. Patients were included in this study if they have medical records of preoperative AP standing knee radiograph, CT image and Knee Society Knee Score [23] (KSKS, an objective knee score completed by the surgeon; details are described in [Supplementary table S2](#)). Patients with valgus alignment, avascular necrosis, poor CT image quality, or congenital or acquired malformations of the femur and tibia were excluded from the study. After selection, 182

patients were included in the analysis. A detailed flowchart of patient selection is shown in [Fig. 1](#). Each patient's demographic information, preoperative KSKS, knee radiograph, and CT data were reviewed retrospectively.

The images for interpretation were taken one week before knee arthroplasty and saved in Digital Imaging and Communications in Medicine (DICOM) format. Imaging parameters of CT data were as follows: thickness 0.625 mm, pixel spacing 0.468750 mm × 0.468750 mm, matrix 512 × 512.

2.2. Radiographic analysis

2.2.1. Radiographic grading of knee osteoarthritis

All patients underwent preoperative AP standing knee radiographs, and the radiographic severity of the knee joint was assessed by an orthopaedics surgeon using the Kellgren-Lawrence grading system [9].

2.2.2. Quantitative measurement of tibial subchondral bone area based on CT images

The 3D models of the femur and tibia were semi-automatically segmented with 3D Slicer (Version 4.10.2, an open-source image processing software). They were transferred into our in-house developed knee quantitative analysis software (Knee-analysis, Ageing Research and Therapy Laboratory, Hong Kong) for quantitative measurement of TSBA and JSW.

We measured the area of the tibial subchondral bone surface based on the region of condyles and intercondylar tubercles concerning the eight anatomic landmarks on the tibia ([Fig. 2a](#)). First, on the top view of the tibia, the points on the boundary of the medial (pink) and lateral (green) tibial subchondral bone were initially marked with label tools ([Fig. 2b](#)). Second, the tibia was rotated to the anterior, posterior, medial, and lateral views ([Fig. 2c](#)) to adjust control points on the medial and lateral plateaus. Third, the triangular 3D medial and lateral bone surfaces ([Fig. 2d](#)) were generated separately from the B-spline contours that enclose the control points. Finally, the area of the two surfaces was calculated as medial and lateral TSBA.

2.2.3. Quantitative measurement of joint space width based on CT images

We measured the 3D JSW of the medial and lateral compartments as the minimum and average projection distances from the triangular surface of the tibial plateau to that of the femoral condyle. The two compartments' projection directions were determined separately by finding the norm of the "best fitting planes" fitted on the tibial subchondral surface using the least square method ([Fig. 3a](#)). In detail, Euclidean distances were measured on the projection lines that start at sampling points with a uniform spacing of 2 mm × 2 mm ([Fig. 3b](#)) and end at the surface of femoral condyles. Sampling points that could not connect to the tibial plateau and femur condyle triangular surface were excluded from the JSW calculations ([Fig. 3c](#)).

2.2.4. Inter-rater and intra-rater reliability measurements

To assess the reliability of TSBA and JSW measurements, 20 knees were randomly selected and independently measured by two examiners to evaluate the inter-observer reliability. One of the examiners repeated the measurements two weeks later for intra-observer analysis.

2.3. Model development

We investigated the classification performance of two parameters, TSBA and JSW, and subsequently developed a CT-based model incorporating these measures. Meanwhile, a clinical model was established, including gender, age, height, weight, BMI, and KSKS. We then established a composite model by combining the CT-based indices and the clinical factors.

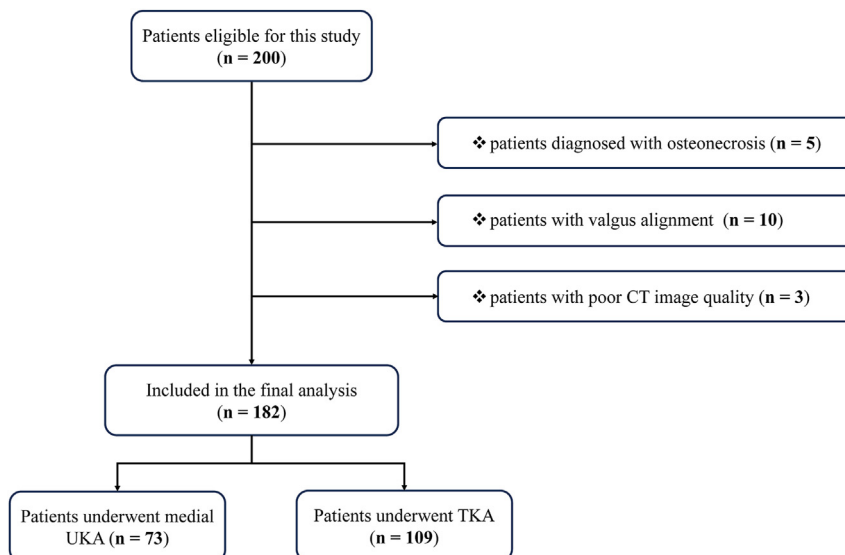


Fig. 1. Flow chart describing the patient enrolment process in this study.

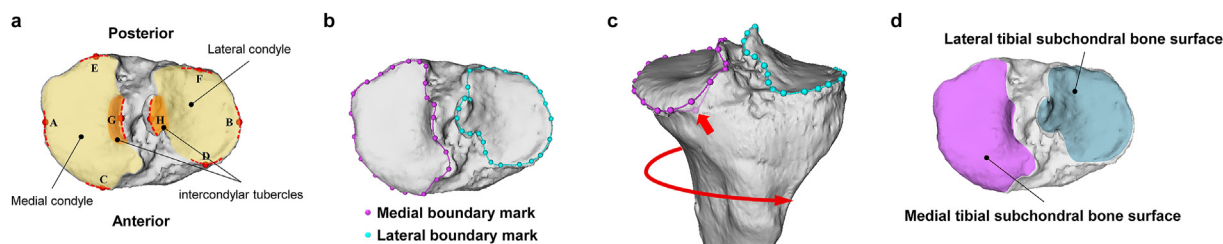


Fig. 2. The workflow of measuring the tibial subchondral bone area. a) the area of the tibial subchondral bone surface measured in this study, points A-F are eight anatomic points: the medial most point of the tibial subchondral bone (point A), the lateral most point of the tibial subchondral bone (point B), the anterior-most point of the medial tibial condyle (point C), the anterior-most point of the lateral tibial condyle (point D), the posterior-most point of the medial tibial condyle (point E), the posterior-most point of the lateral tibial condyle (point F), the medial intercondylar eminence (point G), the lateral intercondylar eminence (point H). b) the initial mark of the boundary of the medial (pink colour) and lateral (green colour) tibial plateau surface. c) the control points were adjusted in different viewing angles manually. d) the medial and lateral tibial subchondral bone surface extracted from the tibia model.

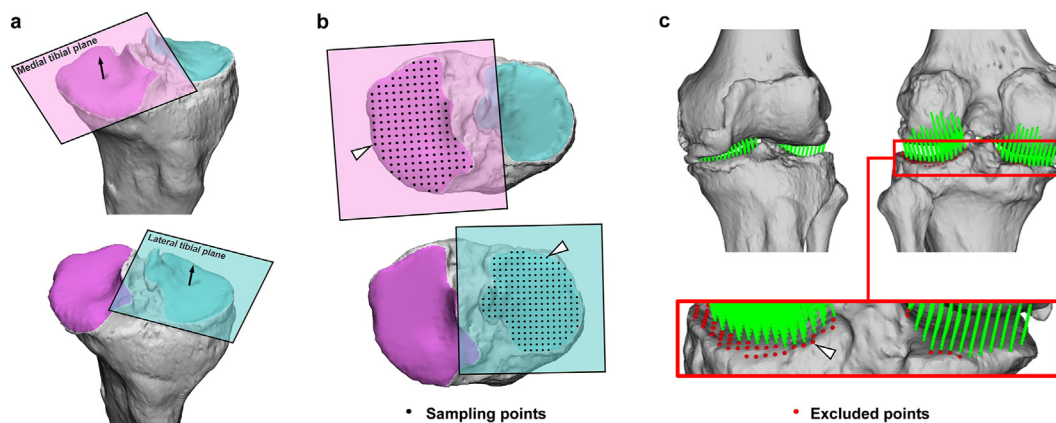


Fig. 3. The workflow of measuring the joint space width. a) the medial and lateral plane fitted by the least square method. b) the sampling points located on the medial and lateral tibial plateau surface. c) the visualization of three-dimensional JSW measured in medial and lateral compartments. The excluded sampling points were marked with red colour.

2.4. Statistical analysis

Descriptive statistics for demographic information of the subjects were tabulated. Independent t-tests were performed for continuous variables and the Chi-Square test was used for categorical variable (gender).

Reliability of the measurement of CT-based parameters, i.e., tibial subchondral bone area and joint space width, were tested using interclass correlation (ICC) [24]. The CT-based parameters in patients with KL grade 3 and patients with KL grade 4 were compared using independent t-tests. The effect of potential confounding factors on the relation

Table 1
Demographical information of subjects.

Characteristics	KL grade 3 (n = 78)	KL grade 4 (n = 104)	p value
Gender (female)	78 (47)	104 (50)	0.139
Age (years)	67.5 (6.2)	66.5 (5.9)	0.370
Height (cm)	157.6 (9.6)	157.5 (7.6)	0.943
Weight (kg)	67.7 (11.8)	67.9 (13.1)	0.956
BMI (kg/m ²)	27.3 (4.2)	27.3 (4.8)	0.996

Values are expressed as means, with SD in parentheses.
Gender differences are compared with the chi-square test.
Abbreviation: KL, Kellgren-Lawrence; BMI, body mass index.

Table 2
Inter-observer and intra-observer reliability.

Parameters	Inter-observer reliability		Intra-observer reliability	
	ICC	95% CI	ICC	95% CI
Medial TSBA	0.992	0.981–0.997	0.987	0.968–0.995
Lateral TSBA	0.986	0.964–0.994	0.988	0.970–0.995
Medial minimal JSW	0.988	0.970–0.995	0.981	0.954–0.993
Lateral minimal JSW	0.966	0.917–0.986	0.989	0.972–0.996
Medial average JSW	0.989	0.973–0.996	0.990	0.974–0.996
Lateral average JSW	0.980	0.975–0.992	0.990	0.975–0.996

Abbreviation: ICC, Intraclass correlation coefficient; CI, Confidence Interval, TSBA, Tibial subchondral bone area; JSW, joint space width.

between CT-based parameters and radiographic severity was explored by calculating estimated marginal means through analysis of variance methods.

The binary logistic regression was performed to determine the effects of CT-based parameters and clinical covariates on the risk that patients underwent TKA. By selecting the significant parameters, all model's formulas are summarised in supplementary. The classification performance of CT-based parameters and the developed models were evaluated using the ROC curves. The Delong test was used to compare the area under the curve (AUC) of different CT-based parameters and the AUCs of different models, respectively.

All statistical analyses were performed using SPSS Statistics (version 26.0; IBM). Two-tailed $p < 0.05$ was considered statistically significant.

3. Results

3.1. Clinical characteristics of patients

A total of 182 patients, 78 patients with KL grade 3 and 104 patients with KL grade 4, were included in the final analysis. The patient demographic information is summarised in Table 1. There were no significant differences in gender distribution, age, height, weight, and body mass index between the two groups.

Table 3
TSBA and JSW in patients with KL grade 3 compared to patients with KL grade 4.

Parameters	Crude analysis ^a			Adjusted analysis ^b		
	KL grade 3 (n = 78)	KL grade 4 (n = 104)	p value	KL grade 3 (n = 78)	KL grade 4 (n = 104)	p value
Medial TSBA (mm ²)	1415.42 (231.42)	1630.59 (258.99)	<0.001	1416.50 (24.46)	1629.82 (20.67)	<0.001
Lateral TSBA (mm ²)	1131.39 (192.38)	1245.87 (221.18)	<0.001	1136.55 (17.88)	1242.18 (15.11)	<0.001
Medial minimal JSW (mm)	1.71 (0.55)	1.25 (0.61)	<0.001	1.72 (0.07)	1.25 (0.06)	<0.001
Lateral minimal JSW (mm)	2.72 (0.83)	2.62 (1.03)	0.472	2.72 (0.11)	2.62 (0.10)	0.931
Medial average JSW (mm)	4.09 (0.89)	3.31 (0.86)	<0.001	4.10 (0.10)	3.31 (0.09)	<0.001
Lateral average JSW (mm)	6.42 (0.98)	6.76 (1.28)	0.075	6.41 (0.13)	6.76 (0.11)	0.058

Abbreviation: TSBA, Tibial subchondral bone area; JSW, joint space width.
The Bold denotes that the results are statistically significant, with a p value < 0.05 .

^a Values are expressed as means, with SD in parentheses.

^b Values are expressed as means, with SE in parentheses, adjusted for age, gender, height, weight, body mass index.

3.2. Parameter reliability test

The inter- and intra-observer reliability of CT-based parameters are shown in Table 2. All parameters showed an almost perfect inter-observer reliability with ICC ≥ 0.966 (95% CI 0.917–0.986). Similarly, an almost perfect intra-observer reliability existed for all parameters with ICC ≥ 0.981 (95% CI 0.954–0.993).

3.3. TSBA and JSW in advanced knee OA patients

Measurements of TSBA, minimal JSW and average JSW in the medial and lateral compartments are summarised in Table 3.

Regarding TSBA, it was found that patients with KL grade 4 had a significantly larger value than those with KL grade 3. In the medial compartment, patients with KL grade 4 (1630.59 ± 258.99 mm²) have 15.2% larger TSBA than those with KL grade 3 (1415.42 ± 231.42 mm², $p < 0.001$). In the lateral compartment, patients with KL grade 4 (1245.87 ± 221.18 mm²) had 10.1 % larger TSBA than those with KL grade 3 (1131.39 ± 192.38 mm², $p < 0.001$). In terms of JSW in the medial compartment, patients with KL grade 4 had smaller minimal JSW and average JSW (1.25 ± 0.61 mm and 3.31 ± 0.86 mm, respectively) than patients with KL grade 3 (1.71 ± 0.55 mm and 4.09 ± 0.89 mm) ($p < 0.001$ for both differences). After adjusting for potential confounding factors (including age, gender, height, weight, and BMI), the results remained significant.

3.4. Univariate and multivariate analyses of classification factors

The clinical characteristics of patients who underwent UKA and TKA are summarised in Supplementary Table S3. Table 4 shows the Odds ratios of patients receiving TKA for twelve classification factors, five of which were statistically significant at univariate analysis: age, BMI, KSKS, medial TSBA, and lateral TSBA. Increases in medial TSBA, lateral TSBA, and BMI were associated with an increased risk of receiving TKA. Conversely, increasing age and KSKS were associated with a decreased risk of receiving TKA.

The multivariate analysis of gender yielded an association with the risk of receiving TKA ($p = 0.034$) but not at univariate analysis ($p = 0.512$). In univariate analysis, BMI, age, and lateral TSBA were associated with the risk of TKA, but not in multivariate analysis. Besides, medial TSBA and KSKS were independent classification factors in both univariate and multivariate analyses ($p \leq 0.001$ for all).

3.5. Performance of TSBA: comparison with JSW

The receiver operating characteristic curve analyses of TSBA, minimal JSW, and average JSW are shown in Fig. 4a. It is shown that medial TSBA yielded an AUC of 0.708, performing the best among those imaging markers, then followed by lateral TSBA (AUC = 0.619). In contrast, the minimal JSW and average JSW yielded the AUCs range from 0.533 to

Table 4
Odds ratios of total knee arthroplasty for classification factors.

Parameters	Univariate		Multivariate	
	Odds Ratio	<i>p</i> value	Odds Ratio	<i>p</i> value
Gender	0.817 (0.446–1.495)	0.512	0.180 (0.037–0.876)	0.034
Age	0.721 (0.530–0.981)	0.037	0.716 (0.436–1.175)	0.186
Height	0.722 (0.514–1.013)	0.059	0.925 (0.030–28.350)	0.965
Weight	1.182 (0.851–1.641)	0.319	0.516 (0.003–89.505)	0.801
BMI	1.544 (1.075–2.219)	0.019	2.086 (0.022–197.731)	0.752
KSKS	0.431 (0.293–0.633)	<0.001	0.305 (0.174–0.536)	<0.001
Medial TSBA	2.217 (1.540–3.191)	<0.001	3.622 (1.708–7.684)	0.001
Lateral TSBA	1.623 (1.163–2.265)	0.004	2.014 (0.890–4.556)	0.093
Medial minimal JSW	0.866 (0.641–1.170)	0.349	1.203 (0.584–2.480)	0.617
Lateral minimal JSW	0.786 (0.581–1.062)	0.117	0.802 (0.460–1.400)	0.438
Medial average JSW	0.813 (0.601–1.098)	0.177	1.021 (0.470–2.216)	0.958
Lateral average JSW	0.893 (0.662–1.203)	0.456	0.607 (0.322–1.147)	0.124

Values in parentheses are 95% confidence intervals.

Gender is for males compared to females.

The Bold denotes that the results are statistically significant, with a *p* value < 0.05.

Abbreviation: KSKS, Knee society knee score; JSW, joint space width; TSBA, Tibial subchondral bone area.

0.554, which were not statistically significantly different from the random classifier (AUC = 0.500). The result suggested that JSW cannot distinguish between UKA patients and those receiving TKA.

A pairwise comparison of AUCs using the DeLong test showed that the performance of medial TSBA is significantly greater than other CT-based parameters (*p* < 0.020 for all); details are presented in [Supplementary Table S4](#).

3.6. Performance of CT-based model: comparison with clinical model

Feature selection for each model using multivariate logistic regression is presented in [Supplementary Table S5](#), with all formulas summarised in [Supplementary](#).

The ROC curves for the three models are shown in [Fig. 4b](#). The composite model demonstrated the highest classification performance (AUC = 0.822). The CT-based model (AUC = 0.708) yielded a classification performance similar to that of the clinical model (AUC = 0.711). A pairwise comparison of AUCs using the DeLong test showed that combining CT-based indices and clinical factors significantly improved classification performance; details are shown in [Supplementary Table S6](#).

4. Discussion

In this study, we performed quantitative measurements of TSBA and JSW on preoperative CT images of patients who underwent primary knee arthroplasty. This study aimed to explore the relation between TSBA and radiographic severity and to determine its performance for classifying surgical decisions between UKA and TKA. We have shown that patients with KL grade 4 have larger medial and lateral TSBA than patients with KL grade 3. These differences remain significant and are not affected by potential confounding factors such as gender, age, or BMI. We also found that TSBA showed greater discrimination in surgical decisions than JSW. Moreover, the Greater classification performance of the composite model, compared with the clinical model and CT-based model, was also demonstrated.

Subchondral bone, a tissue with remodelling capacity that provides mechanical support and nourishment to overlying cartilage [25], adapts to changes in local mechanical loading by altering its contour, shape, and structure [26]. Even in advanced knee OA stages, the subchondral bone's renewal remodelling remains active [18], characterised by decreased bone resorption and sustained bone formation [27]. In this study, as a

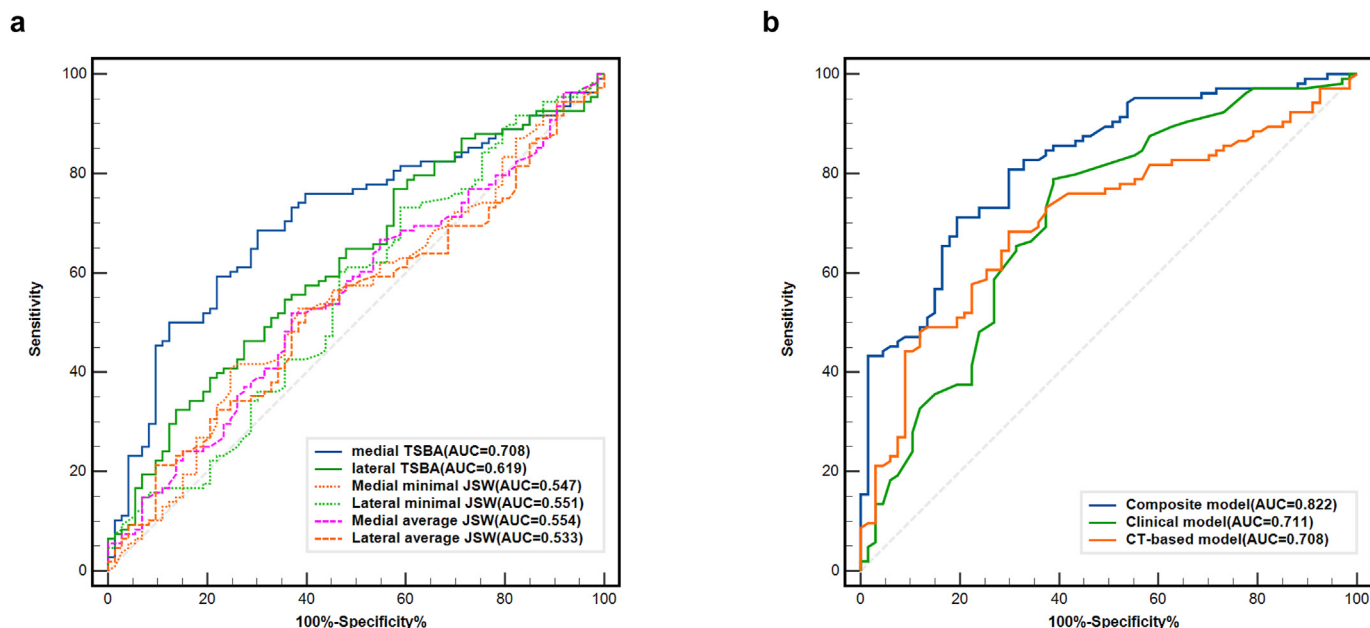


Fig. 4. a) Receiver operating characteristic curves show the performance of TSBA compared to JSW. The classification threshold was 0.50. b) Receiver operating characteristic curves show the performance of the CT-based model compared with the clinical model and composite model. The classification threshold was 0.50.

cumulative consequence of subchondral bone changes, TSBA related to OA radiographic severity showed more pronounced potential than JSW in distinguishing surgical decision-making of advanced knee OA patients. Meanwhile, the result suggests that Medial TSBA is an independent factor associated with surgical decisions. However, BMI, an indication in clinical practice [29], is not significant in multivariate analysis, which may suggest that the effect of BMI on the risk of receiving TKA can be mediated in part through medial TSBA. More studies are needed to investigate the relationship between TSBA and clinical indications further.

Previous quantitative analysis of subchondral bone expansion was mainly based on MRI cross-sectional or sagittal slices [12,13,15]. Although both soft tissue and bone can be visualised in MRI [19], it has been reported recently to underestimate bony structure changes, such as the size of osteophytes [16,17]. For complex bone morphology analysis, CT is preferred as it provides high-resolution 3D images [28]. Furthermore, compared to MRI, CT scans are relatively affordable, time-efficient, and accessible. In clinical practice, several technologies based on CT images have been developed to improve knee replacement surgical accuracies, such as digital surgical planning, patient-specific instrumentation, computer-assisted surgery, and Robotic-Assisted surgery [20,29,30]. The result of this study further expanded the application of CT images in preoperative assessment of the structural severity and surgical decision-making of knee OA.

Our multivariate analysis found gender differences and KSKS to be independent factors of subchondral bone expansion. Females demonstrated a higher risk of requiring TKA than males, partly explained by some previous findings [31,32], such as a higher prevalence of knee OA and a lower pain threshold in females than males. KSKS is the rating of the severity of patient symptoms. Previously, it has been found that there is discordance between radiographic severity and the patient's symptoms [33]. The result of this study supports this consensus, and the composite model (including gender, medial TBSA, and KSKS) is suggested to assist surgical decisions.

The study has several limitations. First, it utilised non-weight-bearing CT images, whereas previous JSW measurements often used weight-bearing radiographs or CT images [7,34]. However, recent research suggests that JSW measurements taken from non-weight-bearing CT scans may provide better correlations with cartilage thickness [35]. Second, we measured only minimum and average JSW, but newer studies examine JSW distribution for additional information [34,36], which could be further compared with TSBA. Third, recent studies reported that the quantitative evaluation of subchondral bone trabecular microstructure based on high-resolution MRI and clinical CT is possible [37,38] and showed a correlation with OA severity. In the future study, we will include both microstructure analysis and more bone shape analysis, such as the slope, concavities, and convexities of the tibial subchondral bone [39,40], to determine their correlation with knee OA severity and explore their application in surgical decision-making for OA patients.

In conclusion, our study results demonstrate that tibial subchondral bone area (TSBA) can reflect radiographic severity in advanced knee OA, and medial TSBA is an independent parameter for classifying surgical decisions between UKA and TKA, outperforming the traditionally used JSW. Further studies are required to validate our findings in other datasets and to translate the results into clinical practice.

Authors contributions

Wei Wang contributed to the conception and design of the study, analysis and interpretation of the data, and drafting of the article. Tianshu Jiang, Jiang Zhang, Jun Liu, Lok Chun Chan, Mengqi Lin, Jia Li contributed to the acquisition and preprocessing of the data, logistic support, and critical revision of the article for important intellectual content. Changhai Ding, Chunyi Wen provided statistical expertise and critical revision of the article. Ping Keung Chan, Kwong Yuen Chiu, Henry Fu and Chunyi Wen contributed to the conception and design of the study and critical revision of the article. Chunyi Wen also provided

administrative and logistic support and funding for this study. All authors gave final approval of the version to be submitted.

Funding statement

This study is supported by the SZRI start-up (I2021A013) and RISports Seed Fund (P0043526), Projects of RISA (P0043001, P0043002), Project of RIAM (P0041372), and Project of Strategic Importance Fund (P0035421) of the Hong Kong Polytechnic University.

Conflict of Interest

The authors have no conflicts of interest relevant to this article.

Acknowledgements

The authors wish to thank Jeffrey Ho Yu Leung, Jin Yan, and Sing Hin Lau for organising patient demographic information. The authors would also like to thank Ziheng Qin and Yilan Lin for segmenting the knee joint.

Appendix A. Supplementary data

Supplementary data to this article can be found online at <https://doi.org/10.1016/j.ocarto.2024.100461>.

References

- [1] A. Cui, H. Li, D. Wang, J. Zhong, Y. Chen, H. Lu, Global, regional prevalence, incidence and risk factors of knee osteoarthritis in population-based studies, *EclinicalMedicine* (2020) 29–30, 100587.
- [2] S.R. Goldring, M.B. Goldring, Changes in the osteochondral unit during osteoarthritis: structure, function and cartilage-bone crosstalk, *Nat. Rev. Rheumatol.* 12 (11) (2016) 632–644.
- [3] O.R. Andrew J Carr, Stephen Graves, Andrew J. Price, Nigel K. Arden, Andrew Judge, David J. Beard, Knee Replacement, *Lancet* 379 (9823) (2012) 1331–1340.
- [4] M. Mikkelsen, H.A. Wilson, K. Gromov, A.J. Price, A. Troelsen, Comparing surgical strategies for end-stage anteromedial osteoarthritis: total versus unicompartmental knee arthroplasty, *Bone Jt Open* 3 (5) (2022) 441–447.
- [5] B. Antony, A. Singh, Imaging and biochemical markers for osteoarthritis, *Diagnostics* (Basel) 11 (7) (2021).
- [6] H. Abdelaziz, O.M. Balde, M. Citak, T. Gehrke, A. Magan, C. Haasper, Kellgren-Lawrence scoring system underestimates cartilage damage when indicating TKA: preoperative radiograph versus intraoperative photograph, *Arch. Orthop. Trauma Surg.* 139 (9) (2019) 1287–1292.
- [7] J.C.-W. Cheung, A.Y.-C. Tam, L.-C. Chan, P.-K. Chan, C. Wen, Superiority of multiple-joint space width over minimum-joint space width approach in the machine learning for radiographic severity and knee osteoarthritis progression, *Biology* 10 (11) (2021).
- [8] M.P. Hellio Le Graverand, S. Mazuca, J. Duryea, A. Brett, Radiographic-based grading methods and radiographic measurement of joint space width in osteoarthritis, *Radiol Clin North Am* 47 (4) (2009) 567–579.
- [9] J.H. Kellgren, J.S. Lawrence, Radiological assessment of osteo-arthrosis, *Ann. Rheum. Dis.* 16 (4) (1957) 494–502.
- [10] A. Guermazi, D. Hayashi, F. Roemer, D.T. Felson, K. Wang, J. Lynch, et al., Severe radiographic knee osteoarthritis—does Kellgren and Lawrence grade 4 represent end stage disease?—the MOST study, *Osteoarthritis Cartilage* 23 (9) (2015) 1499–1505.
- [11] A.R. Sharma, S. Jagga, S.S. Lee, J.S. Nam, Interplay between cartilage and subchondral bone contributing to pathogenesis of osteoarthritis, *Int. J. Mol. Sci.* 14 (10) (2013) 19805–19830.
- [12] C. Ding, F. Cicuttini, G. Jones, Tibial subchondral bone size and knee cartilage defects: relevance to knee osteoarthritis, *Osteoarthritis Cartilage* 15 (5) (2007) 479–486.
- [13] A.E. Wluka, Y. Wang, S.R. Davis, F.M. Cicuttini, Tibial plateau size is related to grade of joint space narrowing and osteophytes in healthy women and in women with osteoarthritis, *Ann. Rheum. Dis.* 64 (7) (2005) 1033–1037.
- [14] M. Hudelmaier, W. Wirth, Differences in subchondral bone size after one year in osteoarthritic and healthy knees, *Osteoarthritis Cartilage* 24 (4) (2016) 623–630.
- [15] G.H. Chang, L.K. Park, N.A. Le, R.S. Jhun, T. Surendran, J. Lai, et al., Subchondral bone length in knee osteoarthritis: a deep learning-derived imaging measure and its association with radiographic and clinical outcomes, *Arthritis Rheumatol.* 73 (12) (2021) 2240–2248.
- [16] X. Liu, Z. Li, Y. Rong, M. Cao, H. Li, C. Jia, et al., A comparison of the distortion in the same field MRI and MR-linac system with a 3D printed phantom, *Front. Oncol.* 11 (2021) 579451.

- [17] F.W. Roemer, K. Engelke, L. Li, J.D. Laredo, A. Guermazi, MRI underestimates presence and size of knee osteophytes using CT as a reference standard, *Osteoarthr. Cartilage* 31 (5) (2023) 656–668.
- [18] H.M. Frost, A 2003 update of bone physiology and Wolff's Law for clinicians, *The Angle orthodontist* 74 (1) (2004) 3–15.
- [19] M.C. Florkow, K. Willemsen, V.V. Mascarenhas, E.H.G. Oei, M. van Stralen, P.R. Seevinck, Magnetic resonance imaging versus computed tomography for three-dimensional bone imaging of musculoskeletal pathologies: a review, *J Magn Reson Imaging* 56 (1) (2022) 11–34.
- [20] A.B. Christ, A.D. Pearle, D.J. Mayman, S.B. Haas, Robotic-assisted unicompartmental knee arthroplasty: state-of-the-art and review of the literature, *J. Arthroplasty* 33 (7) (2018) 1994–2001.
- [21] S.C. Kozinn, R. Scott, Unicompartmental knee arthroplasty, *J Bone Joint Surg Am* 71 (1) (1989) 145–150.
- [22] S.C. Kozinn, C. Marx, R.D. Scott, Unicompartmental knee arthroplasty. A 4.5-6-year follow-up study with a metal-backed tibial component, *J. Arthroplasty* 4 (1989) S1–S10.
- [23] G.R. Scuderi, R.B. Bourne, P.C. Noble, J.B. Benjamin, J.H. Lonner, W.N. Scott, The new knee society knee scoring system, *Clin. Orthop. Relat. Res.* 470 (1) (2012) 3–19.
- [24] V. Rousson, T. Gasser, B. Seifert, Assessing intrarater, interrater and test-retest reliability of continuous measurements, *Stat. Med.* 21 (22) (2002) 3431–3446.
- [25] C.Y. Wen, Y. Chen, H.L. Tang, C.H. Yan, W.W. Lu, K.Y. Chiu, Bone loss at subchondral plate in knee osteoarthritis patients with hypertension and type 2 diabetes mellitus, *Osteoarthr. Cartilage* 21 (11) (2013) 1716–1723.
- [26] S.R. Goldring, Alterations in periarticular bone and cross talk between subchondral bone and articular cartilage in osteoarthritis, *Ther Adv Musculoskelet Dis* 4 (4) (2012) 249–258.
- [27] D.B. Burr, M.A. Gallant, Bone remodelling in osteoarthritis, *Nat. Rev. Rheumatol.* 8 (11) (2012) 665–673.
- [28] D. Wu, M. Sofka, N. Birkbeck, S.K. Zhou, Segmentation of multiple knee bones from CT for orthopedic knee surgery planning, *Med Image Comput Comput Assist Interv* 17 (1) (2014) 372–380.
- [29] I. Dupraz, A. Bollinger, J. Deckx, R.A. Schierjott, M. Utz, M. Jacobs, Using statistical shape models to optimize TKA implant design, *Appl. Sci.* 12 (3) (2022).
- [30] A. Lambrechts, R. Wirix-Speetjens, F. Maes, S. Van Huffel, Artificial intelligence based patient-specific preoperative planning algorithm for total knee arthroplasty, *Front Robot AI* 9 (2022) 840282.
- [31] M. Tschon, D. Contartese, S. Pagani, V. Borsari, M. Fini, Gender and sex are key determinants in osteoarthritis not only confounding variables. A systematic review of clinical data, *J. Clin. Med.* 10 (14) (2021).
- [32] N. Glass, N.A. Segal, K.A. Sluka, J.C. Torner, M.C. Nevitt, D.T. Felson, et al., Examining sex differences in knee pain: the multicenter osteoarthritis study, *Osteoarthr. Cartilage* 22 (8) (2014) 1100–1106.
- [33] E.M. Roos, N.K. Arden, Strategies for the prevention of knee osteoarthritis, *Nat. Rev. Rheumatol.* 12 (2) (2015) 92–101.
- [34] T.D. Turmezei, S. BL, S. Rupret, G.M. Treece, A.H. Gee, J.W. MacKay, et al., Quantitative three-dimensional assessment of knee joint space width from weight-bearing CT, *Radiology* 299 (3) (2021) 649–659.
- [35] M.P. Jansen, S.C. Mastbergen, F. Eckstein, R.J. van Heerwaarden, S. Spruijt, F. Lafeber, Comparison between 2D radiographic weight-bearing joint space width and 3D MRI non-weight-bearing cartilage thickness measures in the knee using non-weight-bearing 2D and 3D CT as an intermediary, *Ther Adv Chronic Dis* 12 (2021) 20406223211037868.
- [36] B. Fritz, J. Fritz, S.F. Fucentese, C.W.A. Pfirrmann, R. Sutter, Three-dimensional analysis for quantification of knee joint space width with weight-bearing CT: comparison with non-weight-bearing CT and weight-bearing radiography, *Osteoarthr. Cartilage* 30 (5) (2022) 671–680.
- [37] C. Liu, C. Liu, X. Ren, L. Si, H. Shen, Q. Wang, et al., Quantitative evaluation of subchondral bone microarchitecture in knee osteoarthritis using 3T MRI, *BMC Musculoskel. Disord.* 18 (1) (2017) 496.
- [38] T. Oláh, X. Cai, L. Gao, F. Walter, D. Pape, M. Cucchiari, et al., Quantifying the human subchondral trabecular bone microstructure in osteoarthritis with clinical CT, *Adv. Sci.* 9 (23) (2022) e2201692.
- [39] Y. Zhang, Y. Chen, M. Qiang, K. Zhang, H. Li, Y. Jiang, et al., Morphometry of the tibial plateau at the surface and resected levels, *J. Arthroplasty* 32 (8) (2017) 2563–2567.
- [40] S. Gong, L.Z. Han, T.L. Gong, Y.H. Yi, R.Y. Wang, W.H. Xu, Correlation between surface area ratio of medial to lateral tibial plateau and knee alignment in adults, *Curr Med Sci* 42 (3) (2022) 577–583.